

Detection of the spin character of Fe(001) surface states by Scanning Tunneling Microscopy: A theoretical proposal

Athanasios N. Chantis,^{1,*} Darryl L. Smith,¹ J. Fransson,² and A. V. Balatsky^{1,3}

¹*Theoretical Division, Los Alamos National Laboratory, Los Alamos, New Mexico 87545, USA*

²*Department of Physics and Materials Science, Uppsala University, Box 530, SE-751 21 Uppsala, Sweden.*

³*Center for Integrated Nanotechnology, Los Alamos National Laboratory, Los Alamos, New Mexico 87545, USA*

(Dated: July 29, 2021)

We consider the magnetic structure on the Fe(001) surface and theoretically study the scanning tunneling spectroscopy using a spin-polarized tip (SP-STM). We show that minority-spin surface states induce a strong bias dependence of the tunneling differential conductance which largely depends on the orientation of the magnetization in the SP-STM tip relative to the easy magnetization axis in the Fe(001) surface. We propose to use this effect in order to determine the spin character of the Fe(001) surface states. This technique can be applied also to other magnetic surfaces in which surface states are observed.

PACS numbers: 72.25.Mk, 73.23.-b, 73.40.Gk, 73.40.Rw

I. INTRODUCTION

The properties of magnetic surfaces and interfaces have attracted recently a lot of attention because of the advent of spintronics, a technology aiming to harness electron's spin in data storage and processing, typically by utilizing heterostructures composed of magnetic and non-magnetic materials¹. Recent theoretical studies revealed that the electronic properties of the Fe(001) surface can play a much more important role for ferromagnet-semiconductor based spintronic devices than it was previously thought^{2,3,4}. Using first-principles electron transport methods it was shown that Fe 3d minority-spin surface (interface) states are responsible for at least two important effects for spin electronics. First, they can produce a *sizable* Tunneling Anisotropic Magnetoresistance (TAMR) in magnetic tunnel junctions with a *single* Fe electrode². The effect is driven by a Rashba shift of the resonant surface band when the magnetization changes direction. This can introduce a new class of spintronic devices, namely, Tunneling Magnetoresistance junctions with a single ferromagnetic electrode⁵ that can function at room temperatures. Second, in Fe/GaAs(001) magnetic tunnel junctions minority-spin interface states produce a *strong* dependence of the tunneling current spin-polarization on applied electrical bias. A dramatic *sign reversal* within a voltage range of just a few tenths of an eV was predicted. This explains the observed sign reversal of spin-polarization in recent experiments of electrical spin injection in Fe/GaAs(001)⁶ and related reversal of tunneling magnetoresistance through vertical Fe/GaAs/Fe trilayers. The TAMR effect was also observed recently in a Fe/GaAs/Au tunnel junction⁷.

Many of the theoretical results mentioned above, are based on theoretical predictions that the Fe(001) surface band is of *minority spin*. However, to this date a *direct* experimental determination of the spin character of the Fe(001) surface band has yet to be done. Scanning tunneling microscopy (STM) is a well established

technique for imaging surface structures^{8,9,10,11} and for spectroscopic measurements of local structures and inhomogeneities on surfaces^{12,13,14}. Using this technique Stroscio *et al* provided the first experimental evidence that a surface band near the Fermi energy exists in the Fe(001) surface¹⁵, however the technique used was incapable of distinguishing the *spin character* of this band. Recent developments of STM tools with spin-polarized tip, SP-STM, allow for controllable measurements of magnetic^{16,17,18} and spin-dynamical¹⁹ features and local magnetic structures²⁰. Spin-polarized tunneling for STM set-up has been theoretically studied with respect to noise²¹, and spin-detection and spin-reversal of local spins located on a substrate surface^{22,23}.

In this paper, we consider a SP-STM set-up on top of a planar Fe surface in order to study the influence of the minority-spin resonant state at the surface on the spin-polarized tunneling current. We found that a complicated angle and energy dependence of the tunneling differential conductance emerges as a result of the energy and momentum dependence of minority-spin band structure in Fe(001) surface. Our results identify a specific route on how to determine the spin character of the Fe(001) surface band with the help of SP-STM. In principle, these results are applicable to a broad set of materials where the minority/majority spin-structure exhibits nontrivial energy dependence.

The rest of this article is organized as follows. In section II we discuss our numerical approach and present our results. Particular emphasis is given to the relation of our approach to Tersoff and Hamman formula for the tunneling current in STM²⁴. Then, based on the obtained results we discuss our proposal on how to detect the spin character of surface states with the help of SP-STM. Section III is the conclusion.

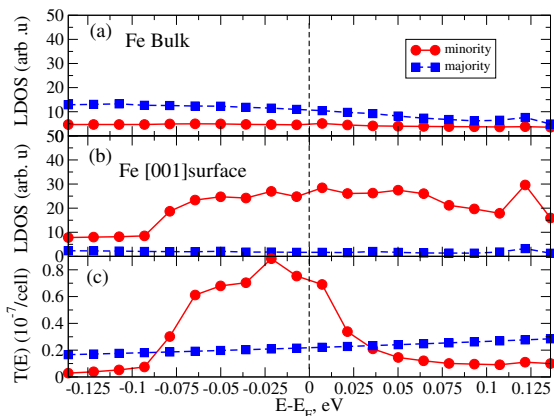


FIG. 1: (a) Spin-resolved DOS for the bulk Fe (b) Spin-resolved DOS for the Fe(001) surface (c) Spin-resolved \mathbf{k}_{\parallel} -integrated transmission for the Fe/vacuum/Cu as a function of energy. The Fermi level is at zero energy.

II. MAIN

We consider a Fe/vacuum/Cu tunnel structure with a nonmagnetic bcc Cu electrode. This electrode has a spin-independent free-electron-like band structure and a featureless surface transmission function²⁵, which makes it insensitive to the transverse wavevector. This electrode simulates an ideal STM tip. The structure investigated consists of a semi-infinite Fe region, several layers of vacuum (empty atomic spheres), and a semi-infinite Cu region. Another advantage of such setup is that it avoids overall the possible 'handshake' of surface resonances at two opposite metallic surfaces/interfaces⁴. When two resonant states on opposite contacts are located in the same $(E, \mathbf{k}_{\parallel})$ space then naturally a resonant transmission equal to 1 will occur across the structure. Obviously a situation like this may occur in a symmetric structure. However, in real structures such 'handshakes' are unlikely because the symmetry of the structure is broken by applied bias or disorder. Therefore, a Fe(001)/vacuum/Fe(001) setup may yield unphysical high transmission for surface states.

The calculation approach is based on the Green's function representation of the Tight-Binding Linear Muffin-Tin Orbital (TB-LMTO) method in the Atomic Sphere Approximation (ASA)²⁶. We use third order parametrization for the Green's function²⁷. The electronic structure problem is solved within the scalar relativistic Density Functional Theory (DFT) where the exchange and correlation potential is treated in the Local Spin Density Approximation (LSDA). The conductance is calculated with the principal-layer Green's function technique^{28,29,30} within the Landauer-Büttiker approach³¹. The semi-infinite Fe and Cu electrodes are separated by approximately 1 nm of vacuum represented by 6 monolayers of empty spheres. The structure is oriented in the [001] direction. Self-consistent charge distribution is achieved before any transport calculations are

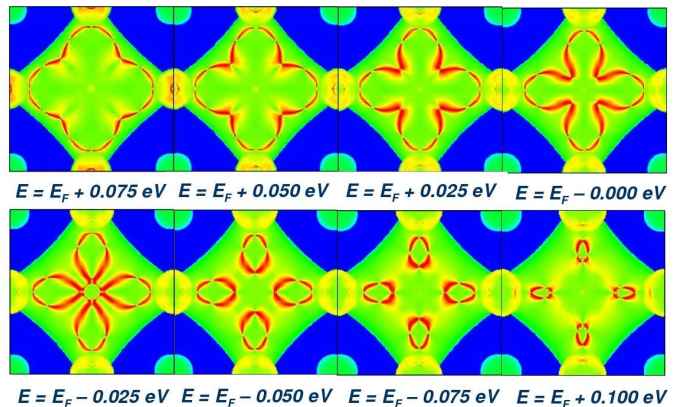


FIG. 2: Minority-spin \mathbf{k}_{\parallel} -resolved DOS of the Fe(001) surface for different energies around the Fermi level. The abscissa is along [100] and the ordinate is along [010]. The maximum value is represented by red color, the minimum by blue.

attempted. The spin-dependent \mathbf{k}_{\parallel} -integrated transmission

$$T^{\sigma}(E) = 1/2\pi \int_{2\text{DBZ}} t^{\sigma}(E, \mathbf{k}_{\parallel}) d^2\mathbf{k}_{\parallel} \quad (1)$$

is calculated in the window from E_F to $E_F + eV$. $t^{\sigma}(E, \mathbf{k}_{\parallel})$ is the transmission coefficient and $\sigma = \uparrow, \downarrow$ (\uparrow =majority-spin, \downarrow =minority-spin). The spin quantization axis lies along (001) direction. A uniform 250×250 mesh was used for the integration in the two-dimensional Brillouin zone (2DBZ). With this transmission we can associate a current density

$$J^{\sigma}(V) = e/h \int_{E_F}^{E_F + eV} T^{\sigma}(E) dE \quad (2)$$

, this is an excellent approximation appropriate for comparison with experiment when the considered voltages are small. Then the spin resolved differential conductance is $dJ^{\sigma}/dV \propto T(E_F + eV)$.

Figs. 1(a) and 1(b) show the calculated Fe bulk spin-resolved density of states (DOS) and Local DOS of the Fe monolayer at the Fe(001) surface, respectively. The energies are given with respect to the Fermi level E_F . In the Fe bulk (Fig. 1(a)) the majority-spin dominates over the minority-spin throughout the entire energy interval shown here. However, in the surface monolayer (Fig. 1(b)) the spin polarization of the DOS is totally reversed; it is the *minority-spin* that dominates over the majority-spin throughout the entire energy interval. In Refs. 2 and 3 it was shown that this reversal is caused by Fe 3d surface states of minority-spin. As shown in Fig. 1(c), sign reversal of the spin polarization of the surface DOS doesn't necessarily lead to sign reversal of the spin polarization of tunneling transmission, at least throughout the same energy interval.

To explain this in Fig. 2 we present the minority-spin \mathbf{k}_{\parallel} -resolved DOS of the Fe(001) surface for different energies around the Fermi level. The bright red features

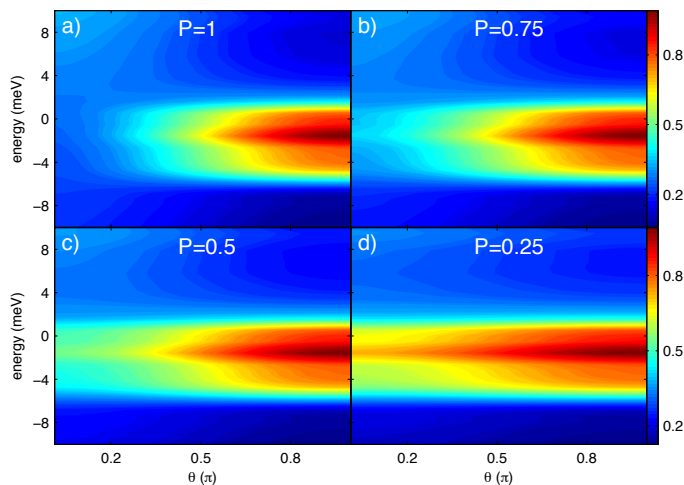


FIG. 3: The energy dependence of the differential conductance of a FM tip as we rotate the direction of the magnetization in the tip by an angle θ relatively to the magnetization in Fe. We show four different cases of DOS spin polarization P of the tip. The bright red regions observed for $\theta = \pi$ are created by the minority spin transmission peaks in Fig. 1(c).

on these plots are created by the surface band. The surface band has C_{4v} symmetry which is the symmetry of the Fe(001) surface. These bands are dominated by the minority-spin surface states arising from $d_{x^2-y^2}$ and d_{xy} orbitals on surface Fe sites that couple with the bulk Fe Δ_2' minority band. Unlike the majority-spin bulk band this band never crosses the 2DBZ at the Γ point. The closer it gets to the Γ point is at the energy of $E_F - 0.025eV$ where we see a bright four-petal structure centered at the Γ point without touching it. Considering that \mathbf{k}_{\parallel} is conserved during tunneling across an ideal surface, for an electron entering the vacuum region with a real \mathbf{k}_{\parallel} the decay rate of the electron wave function is proportional to $\exp\left[-\left(\kappa^2 + \mathbf{k}_{\parallel}^2\right)z\right]$; where κ is the decay rate for normal incidence which is determined by the potential height of the tunneling barrier. The tunneling transmission for a given energy is also proportional to the total number of states at this energy $n_{\sigma}(E)$. In Fig. 1(c) one can compare the spin-resolved tunneling transmission with the spin-resolved surface DOS. We see the influence of both factors just mentioned above in the polarization of the transmission coefficient. The minority-spin transmission dominates over the majority-spin for a large part of the energy interval due to its much higher surface DOS. For the energy $E = E_F - 0.025eV$, the minority-spin transmission has a maximum and in the energy interval where the minority-spin DOS is flat, the minority-spin transmission is less when the surface states are further away from the Γ point. For energies where the minority-spin surface states are far away from the center of the 2DBZ, the minority-spin transmission is less than the majority-spin even though for the same energy the minority-spin surface DOS is much larger than

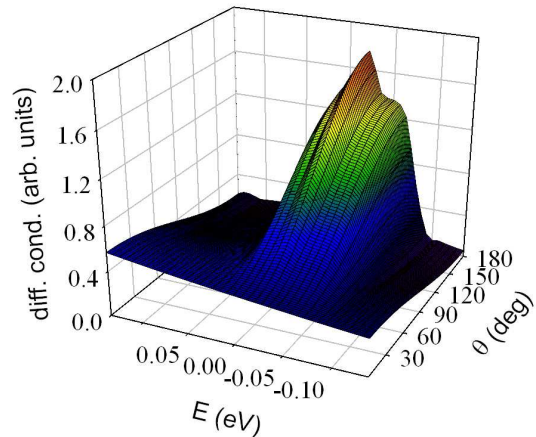


FIG. 4: This is a three dimensional version of Fig3a) ($P=1$)

the majority-spin. For bigger distances between the Cu counterelectrode and the Fe surface the ratio of minority-spin to majority-spin transmission should become even less for all energies in the shown interval. However, our calculations show that for a distance twice as big, the change of spin polarization bias dependence is not very big while the current drops by about four orders of magnitude. This shows that within the range of distances available to an SP-STMTip, the inversion of spin polarization should be detectable (below we describe how).

We connect our results from the planar calculation to the realistic experimental STM set-up by the following observation. Following Tersoff and Hamann²⁴, the tunneling current at 0 K is given by

$$I(V) \propto \sum_{\mathbf{pk}} f(E_i(\mathbf{p})) [1 - f(E_j(\mathbf{k}) - eV)] \times \\ \times |\langle i, \mathbf{p} | T | j, \mathbf{k} \rangle|^2 \delta(E_i(\mathbf{p}) - E_j(\mathbf{k})) \quad (3)$$

where f is the Fermi function and $|\langle i, \mathbf{p} | T | j, \mathbf{k} \rangle|$ is the tunneling matrix element between initial and final states. Here, we designate the momentum index \mathbf{p} (\mathbf{k}) to the Cu tip (Fe substrate) electrons and let i (j) denote the initial (final) state. We take the convention that electrons flow from the tip to the Fe surface for positive voltage V . In our planar case, the role of the tip is played by the Cu surface which, with regards to the tunneling, behaves as an STM tip. Namely, the electronic structure of Cu is known to be relatively featureless around E_F , therefore the tunneling matrix element in Eq. (3) only weakly depends on \mathbf{p} . The substrate surface, on the other hand, has a strong *in-plane* dependence, while the *out-of-plane* component can be written as $\mathbf{k} = \mathbf{k}_{\parallel} + q_z$. By integrating out the \mathbf{p} dependence we can write (3) as

$$I(V) \propto \sum_{\mathbf{k}} [1 - f(E_j(\mathbf{k}) - eV)] f(E_j(\mathbf{k})) |\langle i | T | j, \mathbf{k} \rangle|^2 \propto \\ \int dE \int d\mathbf{k}_{\parallel} [1 - f(E_j(\mathbf{k}) - eV)] f(E_j(\mathbf{k})) |\langle i | T | j, \mathbf{k} \rangle|^2 \quad (4)$$

where in the coefficient of proportionality we have incorporated the density of states of the tip (Cu) at E_F , and the \mathbf{k}_{\parallel} integral is taken in the 2DBZ of Fe surface. Equation (4) is equivalent to Eq. (2), while for a fixed energy Eq. (4) is equivalent to Eq. (1).

Based on these results, we would like to discuss the possibility of detecting the spin-character of Fe surface states with a ferromagnetic (FM) tip. Let's assume that the spin quantization axis in the FM tip is rotated by an angle θ relatively to the spin quantization axis in the Fe surface. The spin components of the electron wave

function in the tip can be written as

$$\begin{aligned} |\uparrow, \theta\rangle &= \cos(\theta/2) |\uparrow\rangle - i \sin(\theta/2) |\downarrow\rangle \\ |\downarrow, \theta\rangle &= -i \sin(\theta/2) |\uparrow\rangle + \cos(\theta/2) |\downarrow\rangle \end{aligned} \quad (5)$$

where, $|\sigma, \theta\rangle$ ($\sigma = \uparrow, \downarrow$) are the spinors for an arbitrary direction of the spin quantization axis and $|\sigma\rangle$ are the spinors for the same spin quantization axis as in Fe. The total transmission coefficient for an arbitrary spin polarization P of the tip can be written as

$$\begin{aligned} T &= (1 + P) T^{\uparrow} \cos^2(\theta/2) + (1 - P) T^{\uparrow} \sin^2(\theta/2) + (1 + P) T^{\downarrow} \sin^2(\theta/2) + (1 - P) T^{\downarrow} \cos^2(\theta/2) \\ &= (T^{\uparrow} + T^{\downarrow}) + (T^{\uparrow} - T^{\downarrow}) P \cos \theta \end{aligned} \quad (6)$$

where, $T^{\uparrow, \downarrow}$ are the spin components of the transmission coefficient (differential conductance) presented in Fig. 1(c). When $\theta = 0$ the spin quantization axis in the tip is parallel to majority-spins in Fe and when $\theta = 180$ it is parallel to minority-spin.

In Fig. 3 we show the energy dependence of the differential conductance of a FM tip as we rotate the direction of the magnetization in the tip by an angle θ relatively to the magnetization in the Fe. Four different cases of DOS spin polarization P of the tip are shown. In the general case, $0 < P < 1$, a complicated energy-angular dependence is observed. However, the trends can be easily understood from the two limiting cases of $P = 1$ (half-metallic tip) and $P = 0$ (not shown in Fig. 3 but can be extrapolated from the case of $P = 0.25$). For $P = 1$ the energy dependence of the transmission for $\theta = 0$ is identical to the majority-spin transmission in Fig. 1(c), while for $\theta = 180$ the energy dependence is identical to that of minority-spin in Fig. 1(c) (to facilitate the comparison in Fig. 4 we provide a three dimensional version of Fig. 3a). As we decrease the degree of spin-polarization in the tip the angular dependence of the differential conductance becomes less pronounced. As it should be, at the limit of $P = 0$ the differential conductance becomes independent of the angle and equal to the sum $T^{\uparrow} + T^{\downarrow}$. This case corresponds to the conventional (non-magnetic tip) STM measurement by Stroscio *et al.*

III. CONCLUSION

In conclusion we have shown that unlike a conventional STM which only can measure a sharp peak in the energy dependence of the differential conductance when a localized surface band is present, an SP-STM measurement should be able to measure an angular dependence as well. In the general case of $0 < P < 1$ a complicated energy-angular dependence emerges but the trends can be easily understood from the limit of a half-metallic, $P = 1$, tip. The energy dependence of the differential conductance in this case will be monotonic for either parallel or anti-parallel direction of the magnetization of the STP tip relative to the direction of the easy axis in the Fe(001) surface. This can be used to extract the spin character of the surface band.

Acknowledgments

The work at Los Alamos National Laboratory was supported by DOE Office of Basic Energy Sciences Work Proposal Number 08SCPE973.

* achantis@lanl.gov

¹ I. Zutic, J. Fabian, and S. D. Sarma, *Reviews of Modern Physics* **76**, 323 (2004).

² A. N. Chantis, K. D. Belashchenko, E. Y. Tsybmal, and M. van Schilfgaarde, *Phys. Rev. Lett.* **98**, 046601 (2007).

³ A. N. Chantis, K. D. Belashchenko, D. L. Smith, E. Y. Tsybmal, M. van Schilfgaarde, and R. C. Albers, *Phys Rev Lett* **99**, 196603 (2007).

⁴ M. N. Khan, J. Henk, and P. Bruno, *J. Phys. Cond. Matter* **20**, 155208 (2008).

⁵ C. Gould, C. Rüster, T. Jungwirth, E. Girgis, G. M. Schott, R. Giraud, K. Brunner, G. Schmidt, and L. W. Molenkamp, *Phys. Rev. Lett.* **93**, 117203 (2004).

⁶ X. Lou, C. Adelman, S. A. Crooker, E. S. Garlid, J. Zhang, K. S. M. Reddy, S. D. Flexner, C. J. Palmstrom, and P. A. Crowell, *Nature Physics* **3**, 197 (2007).

- ⁷ J. Moser, M. Zenger, C. Gerl, D. Schuh, R. Meier, P. Chen, G. Bayreuther, W. Wegscheider, and D. Weiss, *J. Appl. Phys.* **89**, 162106 (2006).
- ⁸ G. Binnig, H. Rohrer, C. Gerber, and E. Weibel, *Appl. Phys. Lett.* **40**, 178 (1981).
- ⁹ G. Binnig, H. Rohrer, C. Gerber, and E. Weibel, *Phys. Rev. Lett.* **49**, 57 (1982).
- ¹⁰ G. Binnig, H. Rohrer, C. Gerber, and E. Weibel, *Phys. Rev. Lett.* **50**, 120 (1983).
- ¹¹ G. Binnig, H. Rohrer, C. Gerber, and E. Weibel, *Surf. Sci.* **131**, L379 (1983).
- ¹² M. F. Crommie, C. P. Lutz, and D. M. Eigler, *Nature* **363**, 524 (1993).
- ¹³ C. F. Hirjibehedin, C. P. Lutz, and A. J. Heinrich, *Science* **312**, 1021 (2006).
- ¹⁴ C. F. Hirjibehedin, C.-Y. Lin, A. F. Otte, M. Ternes, C. P. Lutz, B. A. Jones, and A. J. Heinrich, *Science* **317**, 1199 (2007).
- ¹⁵ J. A. Stroscio, D. T. Pierce, A. Davies, R. J. Celotta, and M. Weinert, *Phys. Rev. Lett.* **75**, 2960 (1995).
- ¹⁶ S. Heinze, M. Bode, A. Kubetzka, O. Pietzsch, X. Nie, S. Blügel, and R. Wiesendanger, *Science* **288**, 1805 (2000).
- ¹⁷ A. Wachowiak, J. Wiebe, M. Bode, O. Pietzsch, M. Morgenstern, and R. Wiesendanger, *Science* **298**, 577 (2002).
- ¹⁸ M. Bode, M. Heide, K. von Bergmann, P. Ferriani, S. Heinze, G. Bihlmayer, A. Kubetzka, O. Pietzsch, S. Blügel, and R. Wiesendanger, *Nature* **447**, 190 (2007).
- ¹⁹ F. Meier, L. Zhou, J. Wiebe, and R. Wiesendanger, *Science* **320**, 82 (2008).
- ²⁰ P. Gambardella, S. Rusponi, M. Veronese, S. S. Dhesi, C. Grazioli, A. Dallmeyer, I. Cabria, R. Zeller, P. H. Dederichs, K. Kern, et al., *Science* **300**, 1130 (2003).
- ²¹ Z. Nussinov, M. F. Crommie, and A. V. Balatsky, *Phys. Rev. B* **68**, 085402 (2003).
- ²² J. Fransson, *Phys. Rev. B* **77**, 205316 (2008).
- ²³ J. Fransson, *Nanotechnology* **19**, 285714 (2008).
- ²⁴ J. Tersoff and D. R. Hamann, *Phys. Rev. B* **31**, 805 (1985).
- ²⁵ K. D. Belashchenko, E. Y. Tsybal, M. van Schilfgaarde, D. A. Stewart, I. I. Oleinik, and S. S. Jaswal, *Phys. Rev. B* **69**, 174408 (2004).
- ²⁶ O. K. Andersen, *Phys. Rev. B* **12**, 3060 (1975).
- ²⁷ O. Gunnarsson, O. Jepsen, and O. K. Andersen, *Phys. Rev. B* **27**, 7144 (1983).
- ²⁸ I. Turek, V. Drchal, J. Kudrnovský, M. Šob, and P. Weinberger, *Electronic structure of disordered alloys, surfaces and interfaces* (Kluwer, 1997).
- ²⁹ J. Kudrnovský, V. Drchal, C. Blaas, P. Weinberger, I. Turek, and P. Bruno, *Phys. Rev. B* **62**, 15084 (2000).
- ³⁰ A. N. Chantis, T. Sandu, and J. L. Xu, *PMC Physics B* **1:13** (2008).
- ³¹ S. Datta, *Electronic transport in mesoscopic systems* (Cambridge University Press, 1995), ch. 3.